Received: 19 June 2023 | Revised: 15 September 2023 | Accepted: 3 October 2023

DOI: 10.1002/pca.3297

RESEARCH ARTICLE

Phytochemical Analysis WILEY

Chemical profiling of botanical extracts obtained in NADES systems using centrifugal partition chromatography combined with ^{13}C NMR dereplication—*Hypericum perforatum* as a case study

Alexis Kotland | **Joseph Thiery** | **Jane Hubert**

NatExplore SAS, Prouilly, France

Correspondence
Jane Hubert, NatExplore SAS, 51140 Prouilly, France.
Email: jane.hubert@nat-explore.com

Funding information
This research received no external funding.

Abstract

Introduction: Natural deep eutectic solvents (NADES) have emerged as interesting extractants to develop botanical ingredients. They are nontoxic and biodegradable, nonflammable, easy to prepare, and able to solubilize a wide range of molecules. However, NADES extracts remain difficult to analyze because the metabolites of interest stay highly diluted in the nonvolatile viscous NADES matrix.

Objective: This study presents a robust analytical workflow for the chemical profiling of NADES extracts. It is applied to *Hypericum perforatum* aerial parts extracted with the neutral mixture fructose/glycerol/water (3/1/1, w/w/w), and compared to the chemical profiling of a classical dry methanol extract.

Methods: Exploiting polarity differences between metabolites, the *H. perforatum* NADES extract was partitioned in a liquid–liquid solvent system to trap the hydrophilic NADES constituents in the lower phase. The upper phase, containing a diversity of secondary metabolites from *H. perforatum*, was fractionated by centrifugal partition chromatography. All fractions were chemically investigated using a ^{13}C NMR dereplication method which involves hierarchical clustering analysis of the whole NMR dataset, a natural metabolite database for metabolite identification, and 2D NMR analyses for validation. Liquid chromatography–mass spectrometry (LC-MS) analyses were also performed to complete the identification process.

Results: A range of 21 metabolites were unambiguously identified, including glycosylated flavonols, lactones, catechins, phenolic acids, lipids, and simple sugars, and 15 additional minor extract constituents were annotated by LC-MS based on exact mass measurements.

Conclusion: The proposed identification process is rapid and nondestructive and provides good prospects to deeply characterize botanical extracts obtained in nonvolatile and viscous NADES systems.

KEYWORDS
chemical profiling, dereplication, extraction, *Hypericum perforatum*, natural deep eutectic solvents, natural products, nuclear magnetic resonance

1 | INTRODUCTION

Recent efforts in the search for new extraction technologies in the field of green chemistry have revealed interesting characteristics of renewable solvents like natural deep eutectic solvents (NADES). NADES refer to mixtures of small natural or naturally derived molecules, usually hydrophilic primary metabolites, which are able to solve metabolites from various chemical classes.[1,2] They naturally occur in plants where they have been hypothesized to play an important role in the biosynthesis and mobilization of bioactive compounds by solubilizing water-insoluble primary and secondary metabolites in the cells.[3] In the laboratory, NADES are prepared by mixing hydrogen bond acceptors, usually amino acids or nontoxic quaternary ammonium salts, with hydrogen bond donors, usually carbohydrates like glucose, fructose, or trehalose, or organic acids like oxalic acid, lactic acid, or malic acid, in specific molar ratios. NADES are always liquid at ambient temperature. They have the particularity to exhibit a much lower melting point than those of the individual constituents due to multiple intermolecular interactions leading to the formation of strong hydrogen bond networks.[4] They are recognized to be nontoxic, biodegradable, and biocompatible. Other advantages are their nonvolatility, chemical and thermal stability, nonflammability, easy preparation, and high extraction capacity.

For all these reasons, NADES have emerged as interesting extractants for the development of food, cosmetic, and pharmaceutical ingredients.[5–8] NADES have been demonstrated as efficient systems to extract various classes of phytochemicals like anthocyanins from blueberry pomace,[9] polyphenols from green tea,[10] steviol glycosides from the leaves of *Stevia rebaudiana*,[11] lutein from the microalga *Scenedesmus* sp.,[12] pigments from spirulina,[13] or ginsenosides from *Panax ginseng*.[14]

But as for all natural extracts, the biological properties governing final applications of NADES extracts strongly depend on their composition in bioactive substances. In this sense the chemical profile of NADES extracts must be carefully assessed to ensure the nontoxicity and quality of the final ingredient. This is where the major analytical challenge directly linked to the intrinsic properties of NADES comes in: Chemical profiling of NADES extracts is often hampered by the low vapor pressure and high viscosity of the NADES matrix, which is very difficult to eliminate for analytical purposes. The metabolites of interest remain highly diluted in the NADES systems, making the purification and identification process a very hard task.

The current study presents a robust analytical workflow for the chemical profiling of botanical extracts when obtained in NADES systems. The method involves a combination of chromatographic, spectroscopic, and data mining tools which was initially developed to accelerate the chemical profiling of natural extracts through nuclear magnetic resonance (NMR)-based dereplication.[15] The workflow starts by centrifugal partition chromatography (CPC) of the crude extract without any loss of biomass, followed by direct NMR analysis of all CPC fractions and organization of the whole NMR dataset by hierarchical clustering analysis (HCA). Metabolite identification is performed with the help of an NMR database dedicated to small natural molecules, which proposes chemical structures potentially matching with the NMR data clusters observed on the HCA heatmap. Database proposals are rigorously validated or reoriented toward the correct solution by manual interpretation of 2D NMR spectra. High-resolution liquid chromatography–mass spectrometry (LC-MS) analyses are also performed to complete the identification process. This approach enables to rapidly obtain a detailed chemical profile without loss of biomass, which means that the starting extract mass can be recovered at the end of the identification process in the form of a well-characterized fraction series. In the last years the robustness of the procedure has been reinforced through many concrete cases of phytochemical investigations conducted on natural extracts of various origins including terrestrial plants and micro- and macroalgae or cultured cell extracts of plant or microbial species.[16–22]

Here, the chemical profile of a NADES extract obtained from the plant species *Hypericum perforatum* was investigated. *H. perforatum* L. (St. John's wort) is a medicinal plant widely used in herbal teas and dietary supplements, mainly to treat depression, anxiety, and insomnia.[23–25] It also exhibits well-recognized anti-inflammatory and antibacterial properties.[26] The active metabolites of *H. perforatum* have been well described in several reports. They include naphtodianthrones, flavonoids, phloroglucinols, and a range of hydroxycinnamic acids.[27–29] Naphtodianthrones in particular, which cover hypericins and pseudohypericins, are typical of the genus *Hypericum* and undoubtedly involved in the pharmacological effects of the medicinal species *H. perforatum*.[27] Phloroglucinol derivatives include the biologically active hyperforins, which also typically occur in *H. perforatum*. Among flavonoids, the glycosides hyperoside and rutin are usually dominating in *Hypericum* species.[27–29]

Our objective was to demonstrate that liquid–liquid extraction followed by CPC fractionation combined with NMR is an efficient approach to chemically profile NADES extracts. *H. perforatum* aerial parts were used as a case study, and the selected NADES was a neutral system composed of fructose, glycerol, and water in the proportions of 3/1/1 (w/w/w). This ternary mixture is fully green, low-cost, renewable, and safe and the constituents are able to interact by H-bonds; therefore, it is relevant for the development of new-generation solvent systems meeting the principles of green chemistry.[30–32] The chemical profile of the *H. perforatum* NADES extract obtained with our analytical strategy was also compared to that of a more classical methanol extract in which the phytochemicals can be easily characterized because the solvent matrix of a methanol extract is 100% removable. Methanol is the most commonly used lab-scale extraction solvent. It is highly polar, volatile, and capable of extracting both lipophilic and hydrophilic substances with good extraction yields. Therefore, it was selected here to produce a dry *H. perforatum* reference extract.

2 | MATERIALS AND METHODS

2.1 | Chemicals and plant material

Fructose was purchased from Sigma-Aldrich (Saint-Louis, USA). OmniPur® glycerol was purchased from Millipore (Merck, Darmstadt,

Germany). Ethyl acetate, acetonitrile, and methanol (MeOH) were purchased from Carlo Erba (Val de Reuil, France). Acetic acid and formic acid were purchased from VWR (Radnor, PA, USA). Deionized water was used to prepare all aqueous solutions. *H. perforatum* aerial parts were manually collected on the summer solstice in June 2022 in a wildflower meadow of Prouilly (Champagne-Ardenne territory, France). On the summer solstice, the aerial parts of *H. perforatum* are mainly composed of opened flowers, leaves, and buds to a lesser extent. After harvest, the plant material was dried for 3 weeks at 25°C away from light and ground into a fine powder using a Microtron MB 550 grinder (Kinematica AG, Switzerland). A voucher specimen of dried *H. perforatum* aerial parts was authenticated by the botanist Professor Laurence Voutquenne-Nazabadioko and deposited in the Herbarium of the Botanical Laboratory at the faculty of Pharmacy of Reims with the label "NAT-HYP-2022" (University of Reims Champagne-Ardenne, Reims, France).

2.2 | NADES system

Fructose, glycerol, and water (FGW) were successively added in the proportions of 3/1/1 (w/w/w) in an Erlenmeyer flask. The mixture was heated at 50°C under magnetic stirring for 1 h. The physicochemical properties of the solvents used to prepare the NADES system are given in Table 1.

2.3 | Preparation of *H. perforatum* extracts

The *H. perforatum* NADES extract was prepared by directly incorporating 20 g of powdered aerial parts into 200 g of the NADES system FGW (3/1/1, w/w/w). Extraction was performed under magnetic stirring for 16 h at room temperature. The resulting mixture was roughly filtered a first time under vacuum through a sintered glass filter (Schott, Zagreb, Croatia) and a second time on a cotton layer. The filtration step was completed with 80 g of fresh NADES, resulting in the final NADES labeled HYP-FGW. In parallel, a conventional methanol extract was prepared by mixing 20 g of powdered *H. perforatum* aerial parts with 200 g of methanol 100% under magnetic stirring overnight (16 h) at room temperature. After filtration on a cotton layer and solvent evaporation, a dry methanol extract of 5.9 g was obtained, named HYP-MeOH (extraction yield = 29.5%).

2.4 | Liquid–liquid extraction and centrifugal partition chromatography

Liquid–liquid partitioning of the NADES extract was performed by solubilizing 40 g of HYP-FGW in 200 mL of the lower phase of the solvent system ethyl acetate/acetonitrile/water (3/3/4, v/v/v) in a separating funnel. Three extraction cycles were performed with 250 mL of fresh upper phase. The three upper phases were combined and evaporated at 50°C to dryness, resulting in 2.0 g of HYP-FGW-UP. The exhausted lower phase was also evaporated to dryness, resulting in 35.8 g of HYP-FGW-LOW. HYP-FGW-UP was then fractionated by CPC using a column of 231mL (CPC-250-PRO from Gilson, Villiers Le Bel, France) connected to a Blueshadow pump 80P (Knauer, Berlin, Germany) and a Labocol Vario 4000 collector (Knauer, Berlin, Germany). The column was made of 12 partition disks engraved with 288 twin cells of ≈1 mL each. The biphasic solvent system was ethyl acetate/acetonitrile/water (3/3/4, v/v/v). The column was filled with the lower phase at 20 mL/min and equilibrated at a rotation speed of 1600 rpm. An aliquot of HYP-FGW-UP (1.8 g) was solubilized in 10 mL of lower phase + 4 mL of upper phase and injected into the CPC column with a 20-mL loop. The mobile phase (upper phase) was eluted for 65 min at 20 mL/min in ascending mode. Then all compounds retained inside the column were recovered by extrusion in descending mode for 10 min, still at 20 mL/min. Fractions of 20 mL were collected from the beginning of elution to the end of extrusion and combined according to their high-performance thin layer chromatography (HPTLC) profiles. HPTLC was performed with a CAMAG® automatic sampler ATS4, a CAMAG® automatic developing chamber ADC2, and a CAMAG® TLC visualizer 2. Fractions were deposited on pre-coated silica gel 60F254 HPTLC Merck plates and eluted with the internally developed migration solvent system ethyl acetate/toluene/acetic acid/formic acid (7/3/1/1, v/v/v/v), visualized under UV light at 254 and 366 nm, and revealed by spraying the dried plates with 50% H_2SO_4 and vanillin followed by heating. As a result, 10 final fractions were obtained from HYP-FGW-UP (Figure 1).

2.5 | NMR analyses and metabolite identification

All dry fractions (up to ≈20 mg when possible in terms of quantity and solubility) were dissolved in 600 µL of DMSO-*d6* and analyzed by ^{13}C NMR at 298 K on a Bruker Avance AVIII-600 spectrometer (Bruker, Karlsruhe, Germany) equipped with a TCI cryoprobe. The uniform driven equilibrium Fourier transform (UDEFT) sequence was

TABLE 1 Physicochemical properties of the solvents used for NADES preparation.

Solvent	N° CAS	Boiling temperature	Vapor pressure (hPa)	Density (g/mL)	Molecular weight (g/mol)
Water	7732-18-5	100°C	23.33 (20°C)	1.0 (25°C)	18.02
Fructose	57-48-7	440°C	-	1.69 (25°C)	180.16
Glycerol	56-81-5	290°C	$<0.1 \times 10^{-3}$ (25°C)	1.261 (20°C)	92.09

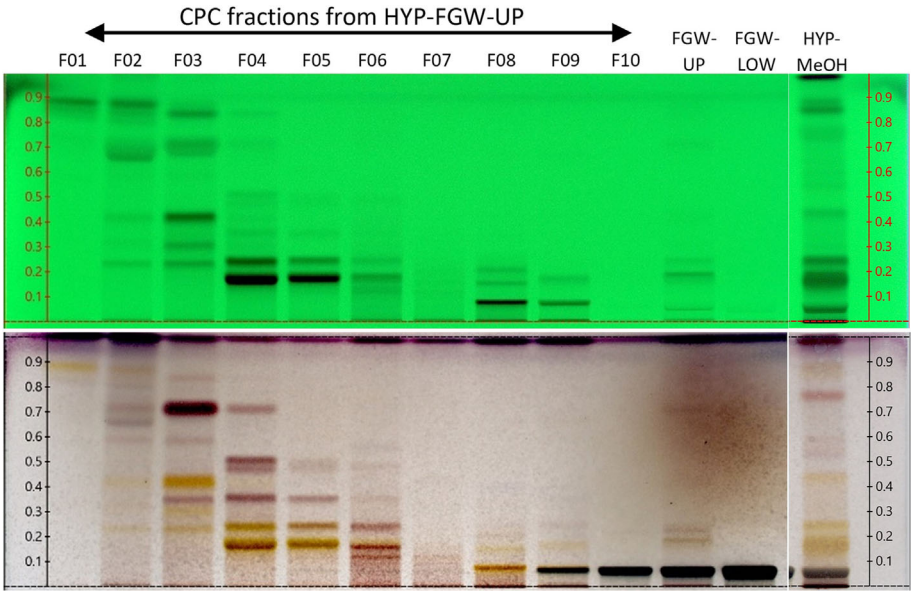

FIGURE 1 TLC profiles of HYP-MeOH, HYP-FGW-LOW, HYP-FGW-UP, and CPC fractions obtained from HYP-FGW-UP at 254 nm (UP) and under visible light after vanillin/H_2SO_4 reagent spraying and heating (down). [Colour figure can be viewed at wileyonlinelibrary.com]

used with an acquisition time of 0.36 s and a relaxation delay of 3 s. The spectral width was 0–240 ppm. A total of 512 scans were recorded to obtain a satisfying signal-to-noise ratio. The receiver gain was set to the highest possible value. All spectra were manually phased, baseline corrected using TOPSPIN 4.0.5 software (Bruker), and calibrated on the central resonance of DMSO-*d6* (δ 39.80 ppm). The absolute intensities of all ^{13}C NMR signals were automatically collected in all spectra of the fraction series and transferred into a table using a locally developed computer script dedicated to NMR signal bucketing with a bucket size of 0.3 ppm. The resulting table was imported into PermutMatrix version 1.9.3 (LIRMM, Montpellier, France) for HCA. In this way, ^{13}C NMR chemical shift clusters were visualized as dendrograms on a 2D map (Figure 2). The higher the intensity of ^{13}C NMR signals, the brighter the color on the map. For metabolite identification, each ^{13}C NMR chemical shift cluster obtained from HCA was manually submitted to a local ^{13}C NMR chemical shift database (interface from ACD/NMR Workbook Suite 2012, ACD/Labs, Ontario, Canada) comprising the structures and predicted chemical shifts of natural molecules ($n \approx 8500$ in April 2023). Additional homonuclear correlation spectroscopy (COSY), heteronuclear single-quantum coherence (HSQC), and heteronuclear multiple bond correlation (HMBC) spectra were also acquired for all fractions to confirm, correct, or further elucidate the chemical structures proposed by the database at the end of the dereplication process. The major metabolites identified in HYP-FGW are presented in Figure 2.

2.6 | High-resolution LC-MS analyses

LC-MS analyses were performed on an Acquity UPLC H-Class system (Waters, Manchester, UK) coupled to a Synapt G2-Si (Waters) equipped with an electrospray ionization (ESI) source. HYP-FGW-LOW, HYP-FGW-UP, and HYP-MeOH were diluted to 10 g/L in methanol/water (50/50, v/v). Chromatographic separation was achieved on an Uptisphere C-18 ODB column (150 × 4.6 mm, 5 µm, Interchim, Montluçon, France). The column temperature was set at 35°C. The sample temperature was maintained at 20°C. Elution was performed using a gradient of water (eluent A) and acetonitrile (eluent B) with 0.1% formic acid in each mobile phase as follows: 0–4 min, 100–74% A; 4–18.5 min, 74–35% A; 18.5–18.7 min, 35–0% A; 18.7–28.7 min, 0% A; 28.7–28.9 min, 0–100% A; 28.9–31 min, 100% A. The flow rate was maintained at 0.7 mL/min. The injection volume was 0.5 µL. MS analyses were performed in negative ion mode (ESI^-). The capillary voltage was 2 kV, the desolvation temperature was 450°C, the desolvation gas flow rate was 950 L/h, the source temperature was 120°C, the cone voltage was 40 V, and the cone gas flow rate was 50 L/h. The mass range for scanning was *m/z* 50–2000.

3 | RESULTS AND DISCUSSION

3.1 | Preparation of the NADES system and *H. perforatum* extracts

In this study, a NADES system was prepared by mixing fructose, glycerol, and water in the proportions of 3/1/1 (w/w/w), resulting in a clear and homogeneous liquid phase, labeled FGW. This ternary mixture contains many hydroxyl units, providing many possibilities to form intermolecular hydrogen bonds and thus favoring the extraction of a large diversity of metabolites.[33] In addition, fructose and glycerol are low-cost, safe, and renewable; therefore, they are relevant green solvents for the preparation of NADES systems and can be safely used in various industrial sectors developing for instance nutraceuticals or natural cosmetic ingredients. The neutrality of the selected NADES system, unlike other common choline-based or acidic NADES systems, is also an important criterion to explore concretely safe applications in such sectors. An FGW mass ratio of 3/1/1 (w/w/w)

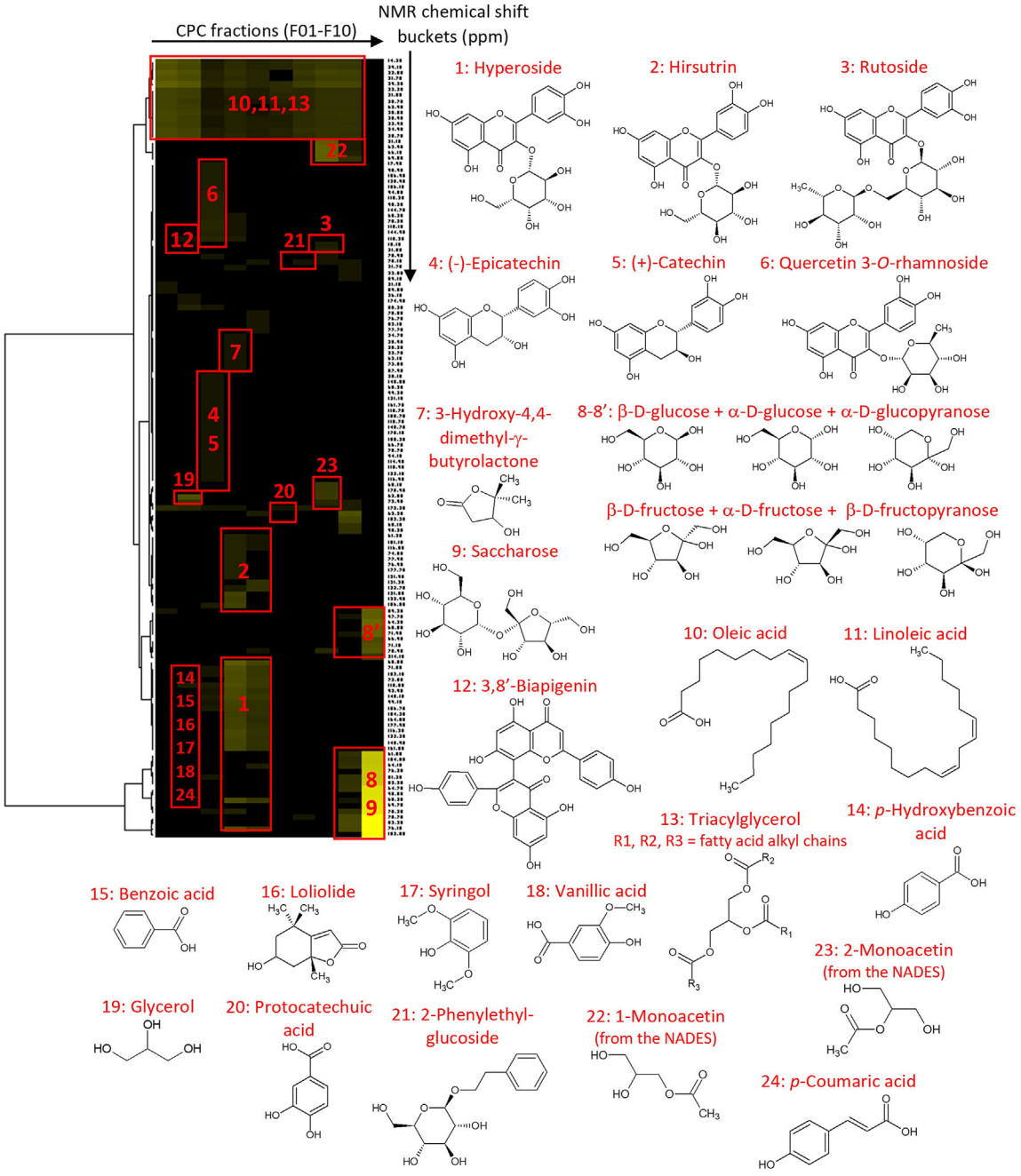

FIGURE 2 HCA heatmap of ^{13}C NMR signals with the identified compounds. [Colour figure can be viewed at wileyonlinelibrary.com]

was selected to obtain a satisfactory solvent system in terms of homogeneity, long-term stability, and extraction capacity. Indeed, it was detailed in a recent paper from Caprin et al.[30] that fructose is poorly soluble in glycerol and an equimolar mixture of both leads to an heterogeneous mixture even at 50°C. Addition of water in this mixture favors the miscibility between constituents and allows the formation of the liquid phase due to its dual role as both H-bond donor and acceptor. It was also shown that ternary mixtures composed of fructose, glycerol, and water are poorly stable over time if the molar ratio between water and fructose is not sufficiently high, with dispersed crystals of fructose progressively appearing after a few weeks at 25°C. Molar ratios between FGW4/4/5 (61/31/8, w/w/w) and FGW1/1/17 (31/16/53, w/w/w) have been revealed necessary to ensure long-term stability of FGW NADES systems with a stable homogeneous liquid phase. Here, therefore, a ternary mixture was selected within this range, composed of fructose, glycerol, and water in the molar proportions of FGW10/6/33 (3/1/1, w/w/w). The resulting NADES extract from *H. perforatum* aerial parts was a yellow and homogenous liquid extract (HYP-FGW). A methanol extract was also prepared in parallel from the same batch of *H. perforatum* and with the same plant/solvent mass ratio of 1/10 (w/w). As a result, a dry extract of 5.9 g (HYP-MeOH) was obtained from 20 g of aerial parts,

corresponding to an extraction yield of 29.5%. The dry methanol extract was red in color.

3.2 | Chemical profiling of the *H. perforatum* NADES extract

The NADES extract HYP-FGW was preliminarily partitioned in the biphasic solvent system ethyl acetate/acetonitrile/water (3/3/4, v/v/v) to concentrate a maximum of *H. perforatum* metabolites of medium polarity in the upper phase while trapping in the lower phase the most hydrophilic constituents including fructose and glycerol from the NADES system and other compounds arising from the primary metabolism of *H. perforatum* like simple sugars or salts. From 40 g of the NADES extract, a dry fraction of 2.0 g was obtained after evaporation of the upper phase (HYP-FGW-UP) and 35.8 g was obtained after evaporation of the lower phase (HYP-FGW-LOW). The total recovery of this liquid–liquid partitioning step was 94.5%. The TLC chemical profiles of HYP-FGW-UP and HYP-FGW-LOW are presented in Figure 1, revealing a more important chemical diversity in the upper phase than in the lower phase. HYP-FGW-LOW only exhibited intense stains of highly hydrophilic constituents eluting below retention factors of 0.1, undoubtedly corresponding in majority to fructose and glycerol from the NADES.

In a context where researchers also start to focus on the recycling of NADES used in bioconversion media, extraction, biomass fractionation, or organic synthesis,[34,35] it might be noted here that liquid–liquid extraction using the biphasic solvent system ethyl acetate/acetonitrile/water (3/3/4, v/v/v) provides interesting perspectives to recycle neutral NADES composed of simple sugars and glycerol. More globally, liquid–liquid partitioning with appropriate solvent systems can be an efficient alternative to solid-phase extraction or membrane-based technology.

HYP-FGW-UP was fractionated by CPC using the same biphasic solvent system ethyl acetate/acetonitrile/water (3/3/4, v/v/v), resulting in a series of 10 final fractions eluted in an increasing order of polarity. The fractionation experiment was rapid; the fraction series was obtained in 80 min only, including elution and extrusion. The TLC profile of the CPC fractions is also presented in Figure 1, revealing a high chemical diversity from F01 to F10 with metabolites from various chemical classes. This also suggested that *H. perforatum* secondary metabolites were well separated from fructose and glycerol of the NADES and highly concentrated in the CPC fractions recovered during elution, making the upcoming NMR-based identification process more manageable.

All CPC fractions were directly analyzed by 1D and 2D NMR, and ^{13}C NMR data were used to build the identification workflow. Automatic picking and bucketing of ^{13}C peaks across the fraction series resulted in a table of 10 columns corresponding to the CPC fractions and 137 rows corresponding to the chemical shift buckets (Δ 0.3 ppm) for which a ^{13}C peak was detected in at least one CPC fraction. This table was submitted to HCA for the recognition of similarities between the ^{13}C NMR fingerprints obtained in successive CPC fractions that could belong to the same molecule. In this way, ^{13}C NMR signals belonging to the constituents of the extract were aggregated as "NMR chemical shift clusters" in a heatmap which is given in Figure 2. The metabolites corresponding to each cluster of the heatmap were identified using an in-house database containing predicted ^{1}H and ^{13}C chemical shift values of natural metabolites ($n \approx 8500$ in May 2023). Database proposals were confirmed or corrected to the right chemical structures by rigorously scrutinizing ^{1}H–^{13}C and ^{1}H–^{1}H correlations in HSQC, HMBC, and COSY spectra. As a result, a total of 21 *H. perforatum* metabolites and three NADES-derived constituents (glycerol, 1-monoacetin, and 2-monoacetin) were unambiguously identified in the NADES extract using this NMR-based identification process. As illustrated in Figure 2, the identified metabolites were

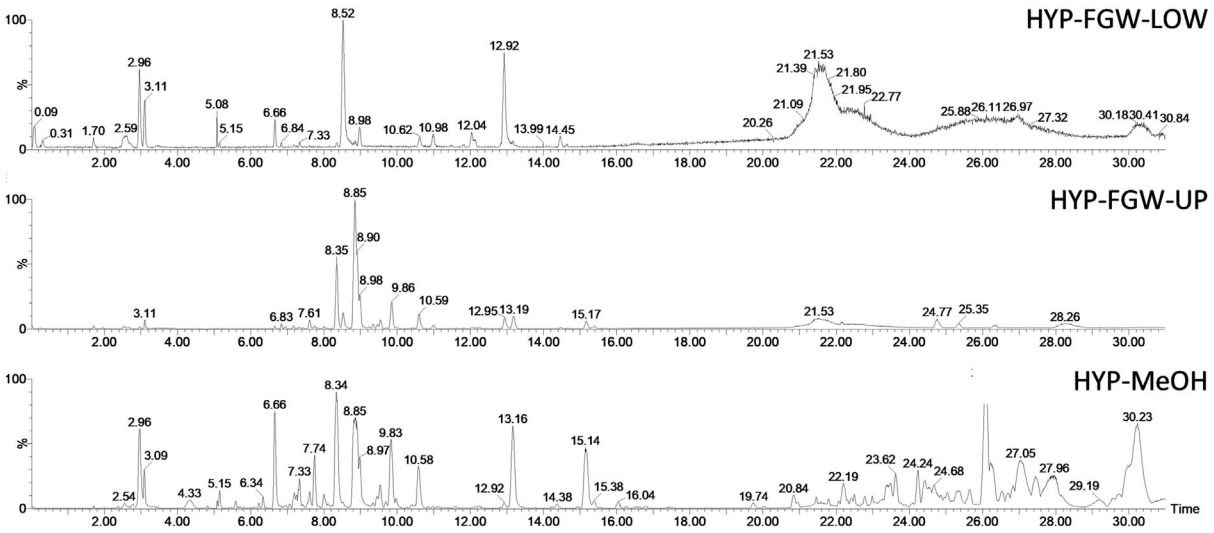

FIGURE 3 LC-MS base peak intensity chromatograms of HYP-FGW-LOW, HYP-FGW-UP, and HYP-MeOH (ESI^-).

TABLE 2 Summary of LC-MS data (ESI-).

HYP-MeOH	FGW-UP	FGW-LOW	LC Retention time (min)	Observed *m/z*	Formula	Δppm	Annotation
×		×	2.96	191.0559	$C_7H_{11}O_6$	1.6	Quinic acid
	×	×	3.09	253.0921	$C_9H_{17}O_8$	−0.8	Glyceryl-hexose (NADES artifact?)
×		×	3.09	341.1085	$C_{12}H_{21}O_{11}$	0.3	Saccharose[a]
×			4.33	233.0662	$C_9H_{13}O_7$	0.4	Not assigned
×		×	5.08	191.0194	$C_6H_7O_7$	1.0	Citric acid
×		×	5.15	233.0662	$C_9H_{13}O_7$	0.4	Not assigned
×			5.59	265.0923	$C_{10}H_{17}O_8$	0.0	Not assigned
×			6.34	315.0720	$C_{13}H_{15}O_9$	1.3	Dihydroxybenzoic acid hexoside
×		×	6.66	353.0879	$C_{16}H_{17}O_9$	1.7	Chlorogenic acid
	×	×	6.84	227.0555	$C_{10}H_{11}O_6$	−0.4	Not assigned
×		×	7.19	353.0876, 191.0560	$C_{16}H_{17}O_9$	0.8	Caffeoylquinic acid (isomer 2)
×			7.25	337.0924, 163.0393, 191.0557	$C_{16}H_{17}O_8$	0.5	Coumaroylquinic acid
×	×		7.32	577.1343, 289.0715	$C_{30}H_{25}O_{12}$	−0.5	Procyanidin dimer
×	×		7.51	865.1978, 431.1919	$C_{45}H_{37}O_{18}$	−0.2	Procyanidin trimer
×	×		7.74	289.0713	$C_{15}H_{13}O_6$	0.3	(+)-Catechin[a] or (−)-epicatechin[a]
×	×		8.00	479.0822	$C_{21}H_{19}O_{13}$	−0.8	Myricetin hexoside or isomer
×	×		8.34	609.1456, 1219.2983	$C_{27}H_{29}O_{16}$	−0.3	Rutoside[a]
×	×		8.52	186.1130	$C_9H_{16}NO_3$	0.0	Not assigned
×	×		8.85	463.0880, 927.1826	$C_{21}H_{19}O_{12}$	−0.5	Hyperoside/hirsutrin[a]
×	×	×	8.97	477.0669, 955.1417	$C_{21}H_{17}O_{13}$	0.0	Quercetin glucuronide
×	×		9.45	447.0923	$C_{21}H_{19}O_{11}$	−0.9	Flavonol hexoside
×	×		9.54	433.0773	$C_{21}H_{17}O_{11}$	0.5	Quercetin pentoside
×	×		9.85	447.0934, 895.1942	$C_{21}H_{19}O_{11}$	1.6	Quercetin rhamnoside[a]
×	×		10.58	505.0984	$C_{23}H_{21}O_{13}$	0.4	Syringetin hexoside or isomer
		×	10.62	186.1132	$C_9H_{16}NO_3$	1.1	Not assigned
	×	×	10.98	187.0969	$C_9H_{15}O_4$	−0.5	Azelaic acid
		×	12.03	512.3332	$C_{26}H_{46}N_3O_7$	−0.8	Not assigned
×	×	×	12.92	526.3494	$C_{27}H_{48}N_3O_7$	0.4	Not assigned
×	×		13.16	301.0348	$C_{15}H_9O_7$	0.0	Quercetin
×			14.38	327.2172	$C_{18}H_{31}O_5$	0.3	C18 fatty acid
	×	×	14.48	527.3328	$C_{27}H_{47}N_2O_8$	−0.8	Not assigned
×	×		15.16	537.0825	$C_{30}H_{17}O_{10}$	0.6	Biapigenin[a] or isomer
×	×		15.38	329.2328	$C_{18}H_{33}O_5$	0.0	C18 fatty acid
×			16.04	537.0823	$C_{30}H_{17}O_{10}$	0.2	Biapigenin[a] or isomer
×			19.74	525.1191	$C_{30}H_{21}O_9$	1.0	Not assigned
×			20.84	699.1354, 519.0715	$C_{36}H_{27}O_{15}$	0.6	Pseudohypericin[b] hexoside
×			21.45	699.1240, 519.0716	$C_{35}H_{25}O_{14}$	−0.6	Pseudohypericin[b] pentoside
×			21.80	331.1905	$C_{20}H_{27}O_4$	−1.2	Empetriferdinan A[b] or isomer
×	×		22.19	303.0141	$C_{14}H_7O_8$	0.0	Not assigned
×			22.49	429.2643	$C_{26}H_{37}O_5$	0.5	Not assigned
×			22.80	615.3537	$C_{35}H_{51}O_9$	0.7	Not assigned
×			23.62	583.3637	$C_{35}H_{51}O_7$	0.3	Not assigned
×			24.24	509.3265	$C_{32}H_{45}O_5$	−0.4	Oxidation product of hyperforin[c]
×			24.43	567.3692	$C_{35}H_{51}O_6$	1.1	Furohyperforin hydroperoxide[b]

(Continues)

TABLE 2 (Continued)

HYP-MeOH	FGW-UP	FGW-LOW	LC Retention time (min)	Observed *m/z*	Formula	Δppm	Annotation
×	×		24.77	271.2277	$C_{16}H_{31}O_3$	1.5	C16 fatty acid
×	×		25.35	1020.6581	-	-	Not assigned
×			26.11	551.3742	$C_{35}H_{51}O_5$	1.1	Hyphenrone A[b]
	×		26.34	1034.6768	-	-	Not assigned
×			27.05	453.3001	$C_{29}H_{41}O_4$	−0.9	Not assigned
×			27.45	613.3745	$C_{36}H_{53}O_8$	0.8	Not assigned
×			27.91	471.3112	$C_{29}H_{43}O_5$	0.4	Not assigned
	×		28.26	537.4886	$C_{34}H_{65}O_4$	0.6	Not assigned
×			30.22	535.3789	$C_{35}H_{51}O_4$	0.4	Hyperforin[b]

[a]Structurally elucidated by NMR.
[b]Already described in the genus *Hypericum* according to https://pubchem.ncbi.nlm.nih.gov/.
[c]Trifunovic et al.[36]

from various chemical families covering a large polarity range, including simple sugars like glucose, fructose, and saccharose, lipidic constituents like triacylglycerols, linoleic acid, or oleic acid, one butyrolactone (3-hydroxy-4,4-dimethyl-γ-butyrolactone), the monoterpene lactone loliolide, (+)-catechin and (−)-epicatechin, syringol, 2-phenylethyl-glucoside, and also a range of highly diverse phenolic acids like vanillic acid, protocatechuic acid, benzoic acid, *p*-coumaric acid, or *p*-hydroxybenzoic acid and various significant mono- and diglycosylated flavonoids mainly derived from quercetin, including hyperoside, hirsutrin, quercetin 3-*O*-rhamnoside, and rutoside, characteristics of the genus *Hypericum*.[25–28] One dimer of apigenin, namely 3,8′-biapigenin, was also identified. It was interesting to observe that even highly diluted in the full NADES extract, CPC fractionation allowed to concentrate *H. perforatum* secondary metabolites in the successive elution fractions F01 to F08, which represented together ≈6.9 wt% of HYP-FGW-UP, corresponding to ≈0.35 wt% of the full NADES extract. On the contrary, the two most polar fractions F09 and F10 recovered by extrusion of the CPC column at the end of the fractionation experiment represented 93.2% of HYP-FGW-UP (≈4.7 wt% of the full NADES extract) and were mainly composed of simple sugars arising from the primary metabolism of the plant.

3.3 | LC-MS comparison of *H. perforatum* extracts: NADES versus MeOH

The NADES sub-extracts (HYP-FGW-UP and HYP-FGW-LOW) and the MeOH extract were analyzed by high-resolution LC-MS in negative ionization mode for a chemical profile comparison. The base peak intensity chromatograms are presented in Figure 3, and LC-MS data are summarized in Table 2. The number of LC peaks observed in the chromatogram of the MeOH extract was higher, particularly in the less polar elution region ranging from 19 to 30 min. Several metabolites derived from hyperforin and hypericin, characteristic of the genus *Hypericum*, were detected in HYP-MeOH only. This indicates that the NADES system used in this work is not very suitable to extract such nonpolar compounds. This could be explained by the poor capability of hyperforin derivatives to form intermolecular H-bonds with the NADES due to the absence of favorable groups, most decorative units on the hyperforin skeleton being neutral dimethyl allyl units. For hypericin derivatives, one can hypothesize that the naphthodianthrone structure is maybe too rigid to form intermolecular H-bonds with the NADES. In the elution region from 2 to 18 min, most peaks detected in the LC chromatogram of HYP-MeOH were also detected in HYP-FGW-UP or HYP-FGW-LOW, indicating close chemical profiles regarding metabolites of medium and high polarity. Several NADES extract constituents identified by NMR were also detected by LC-MS, namely saccharose, (+)-catechin and (−)-epicatechin, rutoside, hyperoside, hirsutrin, quercetin 3-*O*-rhamnoside, and 3,8′-biapigenin. In addition to the 21 compounds unambiguously identified by NMR, several NADES extract constituents were additionally detected by LC-MS, which is a more sensitive detection technique than NMR. These additional compounds were minor constituents of HYP-FGW-UP and HYP-FGW-LOW. They include quinic acid, citric acid, a dihydroxybenzoic acid hexoside, chlorogenic acid and another caffeoylquinic acid isomer, a coumaroylquinic acid, two procyanidin dimers, a myricetin hexoside, a quercetin glucuronide, a quercetin pentoside, a syringetin hexoside, azelaic acid, quercetin, and a second biapigenin isomer. These 15 compounds were annotated based on exact mass measurements and thus their identification was only putative.

In summary, this study has presented a powerful analytical strategy for the nontargeted chemical profiling of botanical extracts when prepared with neutral NADES systems. Many metabolites from *H. perforatum* aerial parts were successfully extracted with the stable ternary mixture fructose/glycerol/water (3/1/1, w/w/w). In comparison to the so far therapeutically accepted hydroalcoholic solvents (EtOH/H_2O) for the extraction of *H. perforatum* aerial parts, NADES technology offers interesting prospects to develop botanical ingredients. Further toxicological investigations would be required to incorporate NADES as a standard technology in this field. From an

analytical point of view, exploiting the polarity range of extract constituents, judicious coordinated steps of liquid–liquid extraction and fractionation allowed to separate the abundant NADES components fructose and glycerol from the metabolites of interest belonging to the plant. A total of 21 phytochemicals were unambiguously identified using the NMR-based identification process, and 15 additional minor extract constituents were annotated by LC-MS based on exact mass measurements. This chemical profiling approach is rapid and nondestructive. A detailed chemical map of the *H. perforatum* NADES extract was obtained.

ACKNOWLEDGMENTS

We thank the University of Reims Champagne-Ardenne (URCA) for providing access to the Analytical Platform PlAneT for NMR and high-resolution LC-MS analyses. We also thank Professor Laurence Voutquenne-Nazabadioko from the Laboratory of Botany of URCA for the authentication of *H. perforatum* aerial parts.

DATA AVAILABILITY STATEMENT

The data that support the findings of this study are available from the corresponding author upon request.

ORCID

Jane Hubert https://orcid.org/0009-0000-5713-9327

REFERENCES

1. Dai Y, Witkamp GJ, Verpoorte R, Choi YH. Natural deep eutectic solvents as new extraction media for phenolic metabolites in safflower. *Anal Chem*. 2013;85(13):6272-6278. doi:10.1021/ac400432p
2. Cao J, Cao J, Wang H, Chen L, Cao F, Su E. Solubility improvement of phytochemicals using (natural) deep eutectic solvents and their bioactivity evaluation. *J Mol Liq*. 2020;318:113997. doi:10.1016/j.molliq.2020.113997
3. Choi YH, Van Spronsen J, Dai Y, et al. Are natural deep eutectic solvents the missing link in understanding cellular metabolism and physiology? *Plant Physiol*. 2011;156(4):1701-1705. doi:10.1104/pp.111.178426
4. Durand E, Lecomte J, Villeneuve P. From green chemistry to nature: the versatile role of low transition temperature mixtures. *Biochimie*. 2016;120:119-123. doi:10.1016/j.biochi.2015.09.019
5. Rente D, Bubalo MC, Panić M, et al. Review of deep eutectic systems from laboratory to industry, taking the application in the cosmetics industry as an example. *J Clean Prod*. 2022;380, Part 2:135147. doi:10.1016/j.jclepro.2022.135147
6. Cannavacciuolo C, Pagliari S, Frigerio J, Giustra CM, Labra M, Campone L. Natural deep eutectic solvents (NADESs) combined with sustainable extraction techniques: a review of the green chemistry approach in food analysis. *Foods*. 2022;12(1):56. doi:10.3390/foods12010056
7. Wils L, Hilali S, Boudesocque-Delaye L. Biomass valorization using natural deep eutectic solvents: what's new in France? *Molecules*. 2021;26(21):6556. doi:10.3390/molecules26216556
8. Duru KC, Slesarev GP, Aboushanab SA, et al. An eco-friendly approach to enhance the extraction and recovery efficiency of isoflavones from kudzu roots and soy molasses wastes using ultrasound-assisted extraction with natural deep eutectic solvents (NADES). *Ind Crops Prod*. 2022;182:114886. doi:10.1016/j.indcrop.2022.114886
9. Fu X, Wang D, Belwal T, et al. Natural deep eutectic solvent enhanced pulse-ultrasonication assisted extraction as a multi-stability protective and efficient green strategy to extract anthocyanin from blueberry pomace. *LWT*. 2021;144:111220. doi:10.1016/j.lwt.2021.111220
10. Cui Z, Djocki Enjome AV, Yao J, et al. COSMO-SAC-supported evaluation of natural deep eutectic solvents for the extraction of tea polyphenols and process optimization. *J Mol Liq*. 2021;328:115406. doi:10.1016/j.molliq.2021.115406
11. Suresh PS, Singh PP, Sharma M, Sharma U. Multicomponent natural deep eutectic solvents: super solvents for the efficient extraction of steviol glycosides (rebaudioside a) from *Stevia rebaudiana*. *J Clean Prod*. 2023;385:135639. doi:10.1016/j.jclepro.2022.135639
12. Fan C, Liu Y, Shan Y, Cao X. A priori design of new natural deep eutectic solvent for lutein recovery from microalgae. *Food Chem*. 2022;376:131930. doi:10.1016/j.foodchem.2021.131930
13. Wils L, Leman-Loubière C, Bellin N, et al. Natural deep eutectic solvent formulations for spirulina: preparation, intensification, and skin impact. *Algal Research*. 2021;56:102317. doi:10.1016/j.algal.2021.102317
14. Jeong KM, Lee MS, Nam MW, et al. Tailoring and recycling of deep eutectic solvents as sustainable and efficient extraction media. *J Chromatogr a*. 2015;1424:10-17. doi:10.1016/j.chroma.2015.10.083
15. Hubert J, Nuzillard JM, Purson S, et al. Identification of natural metabolites in mixture: a pattern recognition strategy based on (13)C NMR. *Anal Chem*. 2014;86(6):2955-2962. doi:10.1021/ac403223f
16. Abedini A, Colin M, Hubert J, et al. Abundant extractable metabolites from temperate tree barks: the specific antimicrobial activity of *Prunus Avium* extracts. *Antibiotics*. 2020;9(3):111. doi:10.3390/antibiotics9030111
17. Hammoud Mahdi D, Hubert J, Renault JH, et al. Chemical profile and antimicrobial activity of the fungus-growing termite strain *Macrotermes bellicosus* used in traditional medicine in the Republic of Benin. *Molecules*. 2020;25(21):5015. doi:10.3390/molecules25215015
18. Angelis A, Hubert J, Aligiannis N, et al. Bio-guided isolation of methanol-soluble metabolites of common spruce (*Picea abies*) bark by-products and investigation of their dermo-cosmetic properties. *Molecules*. 2016;21(11):1586. doi:10.3390/molecules21111586
19. Darme P, Spalenka J, Hubert J, et al. Investigation of antiparasitic activity of ten European tree bark extracts on *toxoplasma gondii* and bioguided identification of triterpenes in *Alnus glutinosa* barks. *Antimicrob Agents Chemother*. 2022;66(1):e0109821. doi:10.1128/AAC.01098-21
20. Hubert J, Kotland A, Henes B, Poigny S, Wandrey F. Deciphering the phytochemical profile of an Alpine rose (*Rhododendron ferrugineum* L.) leaf extract for a better understanding of its Senolytic and skin-rejuvenation effects. *Cosmetics*. 2022;9(2):37, 37. doi:10.3390/cosmetics9020037
21. Favre-Godal Q, Hubert J, Kotland A, et al. Extensive phytochemical assessment of *Dendrobium fimbriatum* hook (Orchidaceae). *Nat Prod Commun*. 2022;17(3):1934578X2210745. doi:10.1177/1934578X221074526
22. Grigolon G, Nowak K, Poigny S, et al. From coffee waste to active ingredient for cosmetic applications. *Int J Mol Sci*. 2023 May 10;24(10):8516. doi:10.3390/ijms24108516
23. Kasper S, Caraci F, Forti B, Drago F, Aguglia E. Efficacy and tolerability of *Hypericum* extract for the treatment of mild to moderate depression. *Eur Neuropsychopharmacol*. 2010;20(11):747-765. doi:10.1016/j.euroneuro.2010.07.005
24. Galeotti N. *Hypericum perforatum* (St John's wort) beyond depression: a therapeutic perspective for pain conditions. *J Ethnopharmacol*. 2017;200:136-146. doi:10.1016/j.jep.2017.02.016
25. Zhang R, Ji Y, Zhang X, Kennelly EJ, Long C. Ethnopharmacology of *Hypericum* species in China: a comprehensive review on ethnobotany,

phytochemistry and pharmacology. *J Ethnopharmacol*. 2020;254:112686. doi:10.1016/j.jep.2020.112686
26. Saddiqe Z, Naeem I, Maimoona A. A review of the antibacterial activity of *Hypericum perforatum* L. *J Ethnopharmacol*. 2010;131(3):511-521. doi:10.1016/j.jep.2010.07.034
27. Napoli E, Siracusa L, Ruberto G, et al. Phytochemical profiles, phototoxic and antioxidantproperties of eleven *Hypericum* species: a comparative study. *Phytochemistry*. 2018;152:162-173. doi:10.1016/j.phytochem.2018.05.003
28. Patocka J. The chemistry, pharmacology, and toxicology of the biologicallyactive constituents of the herb *Hypericum perforatum* L. *J Appl Biomed*. 2003;1:61-70. doi:10.32725/jab.2003.010
29. Carrubba A, Lazzara S, Giovino A, Ruberto G, Napoli E. Content variability of bioactive secondary metabolites in *Hypericum perforatum* L. *Phytochem Lett*. 2021;46:71-78. doi:10.1016/j.phytol.2021.09.011
30. Caprin B, Charton V, Rodier JD, et al. Scrutiny of the supramolecular structure of bio-sourced fructose/glycerol/water ternary mixtures: towards green low transition temperature mixtures. *J Mol Liq*. 2021;337:116428. doi:10.1016/j.molliq.2021.116428
31. Gu Y, Jérôme F. Glycerol as a sustainable solvent for green chemistry. *Green Chem*. 2010;12(7):1127. doi:10.1039/C001628D
32. Jablonský M, Škulcová A, Malvis A, Šima J. Extraction of value-added components from food industry based and agro-forest biowastes by deep eutectic solvents. *J Biotechnol*. 2018;282:46-66. doi:10.1016/j.jbiotec.2018.06.349
33. Benvenutti L, Ferreira Zielinski AA, Salvador Ferreira SR. Which is the best food emerging solvent: IL, DES or NADES? *Trends Food Sci Technol*. 2019;90:133-146. doi:10.1016/j.tifs.2019.06.003
34. Li M, Rao C, Ye X, et al. Applications for natural deep eutectic solvents in Chinese herbal medicines. *Front Pharmacol*. 2023;13:1104096. doi:10.3389/fphar.2022.1104096
35. Liang X, Zhang J, Huang Z, Guo Y. Sustainable recovery and recycling of natural deep eutectic solvent for biomass fractionation via industrial membrane-based technique. *Ind Crops Prod*. 2023;194:116351. doi:10.1016/j.indcrop.2023.116351
36. Trifunović S, Vajs V, Macura S, et al. Oxidation products of hyperforin from *Hypericum perforatum*. *Phytochemistry*. 1998;49(5):1305-1310. doi:10.1016/s0031-9422(97)00903-5

SUPPORTING INFORMATION

Additional supporting information can be found online in the Supporting Information section at the end of this article.

How to cite this article: Kotland A, Thiery J, Hubert J. Chemical profiling of botanical extracts obtained in NADES systems using centrifugal partition chromatography combined with ^{13}C NMR dereplication—*Hypericum perforatum* as a case study. *Phytochemical Analysis*. 2023;1-10. doi:10.1002/pca.3297